

## Dynamic Kingdon trap

R. Blümel

*Department of Physics, State University of New York, Stony Brook, New York 11794-3800*

(Received 15 September 1994)

The dynamic Kingdon trap is a trap designed for the permanent storage of charged particles. While the Paul trap is based on the principle of strong focusing, the dynamic Kingdon trap uses strong defocusing to achieve trapping. It is shown that the dynamic Kingdon trap exhibits a sequence of period-doubling bifurcations. A numerical solution of the Laplace equation for a finite-length dynamic Kingdon trap with holding caps shows that this trap can be implemented in the laboratory.

PACS number(s): 32.80.Pj, 65.45.+b

The static Kingdon trap, an ion trap consisting of nothing more than a metal filament surrounded by a metal cylinder, was described early in the literature [1]. This trap is simple and robust and has one important advantage: it works with a static voltage applied between the cylinder and the filament. In the absence of collisions and neglecting radiative effects, this trap is able to “imprison” [1] a charged particle for an indefinite period of time. It has one disadvantage: the particle has to orbit the filament, for if it had no angular momentum component in the direction of the filament, it would quickly be captured by the filament and discharge. But if an ac voltage is added to the dc voltage, stable trapping can be achieved even for zero angular momentum with respect to the filament; the simple static Kingdon trap becomes the *dynamic Kingdon trap*. It is a close relative of the Paul trap [2,3], but there are important differences as we shall see below. We will now discuss an ideal cylindrical version of the dynamic Kingdon trap with infinite length. A realistic trap of finite length will be discussed later.

A superposition of an ac and a dc voltage applied between the filament and the outer cylinder of the trap results in a charge density (charge per unit length)

$$\sigma = \sigma_{dc} + \sigma_{ac} \cos(\Omega t) \quad (1)$$

on the filament. The electric field between the filament and the outer cylinder points into the radial direction. Its magnitude is given by

$$E = \sigma/2\pi\epsilon_0 r, \quad (2)$$

where  $r$  is the distance from the filament. In the absence of an initial velocity component perpendicular to the  $r$  direction, the motion of an ion with mass  $m$  and charge  $Z$  in this field will be one-dimensional in the  $r$  direction, and a single scalar equation suffices to describe the ion dynamics:

$$m\ddot{r} = ZE = Z\sigma/2\pi\epsilon_0 r. \quad (3)$$

Introducing dimensionless time  $\tau = \Omega t/2$  and a unit of length  $l$  such that

$$\left| \frac{2Z\sigma_{dc}}{m\Omega^2\pi\epsilon_0 l^2} \right| = 1, \quad (4)$$

the equation of motion for  $r$  reads

$$\ddot{r} + [s - 2\eta\cos(2\tau)]\frac{1}{r} = 0, \quad (5)$$

where  $s$  (according to the relative polarities of  $Z$  and  $\sigma_{dc}$ ) can take the values  $\pm 1$  and  $\eta = \sigma_{ac}/2\sigma_{dc}$ . Equation (5) looks very similar to a Mathieu equation [4], but it is nonlinear. It may be called the “Kingdon equation.” I am not currently aware of a systematic study of the Kingdon equation in the mathematical literature, but a physical approach based on the notion of the pseudopotential [5] provides already some valuable insight into the properties of (5).

The essence of the pseudopotential approach is to replace a rapidly oscillating inhomogeneous force field with a static force (also known as the “ponderomotive force”) that can be derived from a time-independent “pseudopotential.” The idea is that on average the pseudopotential has the same effect as the time-dependent field. The method is discussed in standard textbooks [6,7]. The net result is the following: Suppose a particle of mass  $m$ , moving in one dimension  $x$ , is subjected to a rapidly oscillating force  $f(x,t) = f_0(x)\cos(\omega t)$ . Then, to a good approximation, the average force acting on the particle can be obtained as the negative gradient of the pseudopotential  $U_{eff}(x) = f_0^2(x)/4m\omega^2$ . Because of the fast residual components of the force, not taken into account in the pseudopotential, the particle will execute rapid oscillations around its average path determined by  $U_{eff}$ . This oscillatory motion is called the “micromotion” [2,3,5]. Its amplitude  $\xi$  can be estimated according to [6,7] as  $\xi = |f_0(x)|/m\omega^2$ . According to these results the total pseudopotential for (5) (including the static potential) is given by

$$U_{eff}(r) = s\ln(r) + \eta^2/4r^2, \quad (6)$$

and the micromotion amplitude is given by

$$\xi = \eta/2r. \quad (7)$$

Interpreting (6) we see that the effect of the ac voltage is to drive the ion away from the central filament of the trap and toward the outer cylinder. Thus, the effect of the ac voltage is *destabilizing*, or in the language of accelerator physics (see, e.g., [8]), the effect is one of *strong defocusing*. In order to counterbalance the defocusing effect, the dc voltage applied to the trap has to be chosen such that the ion is attracted

TABLE I. Equilibrium values of  $r_0$  (column 2),  $r_0/\eta$  (column 3), and  $\xi$  (column 4) for a single ion stored in a dynamic Kingdon trap for various values of the control parameter  $\eta$  (column 1) and damping constant  $\gamma=10^{-3}$ .

$\eta$	$r_0$	$r_0/\eta$	$\xi$
4	2.889	0.722	0.7073
6	4.283	0.714	0.7072
8	5.687	0.711	0.7071
10	7.095	0.710	0.7071

toward the filament. This is equivalent to the choice  $s=1$ , while for  $s=-1$  both the ac and the dc voltage conspire to drive the ion toward the outer cylinder of the trap. In other words, stable trapping is possible only if (6) exhibits a potential minimum. For  $s=-1$  no such minimum exists. The trap is globally unstable. For  $s=1$ , however, (6) always possesses a potential minimum located at

$$r_0 = \eta/\sqrt{2}. \quad (8)$$

The micromotion amplitude at the minimum is given by

$$\xi = \eta/2r_0 = 1/\sqrt{2}. \quad (9)$$

Summarizing, the pseudopotential picture predicts the following scenario for  $s=1$ . In the presence of a cooling mechanism (buffer gas, or laser cooling) a charged particle in the dynamic Kingdon trap will settle down close to the pseudopotential minimum  $r_0$  of the trap, executing small oscillations of magnitude  $\xi$  around this equilibrium position. Thus, the main result of the pseudopotential analysis is that the dynamic Kingdon trap is indeed a working device for the stable trapping of charged particles.

In order to check the pseudopotential picture, and to rigorously demonstrate the working principle of the dynamic Kingdon trap in the presence of the micromotion, numerical simulations of a dynamic Kingdon trap were performed. Cooling was simulated by adding a damping term to (5). This way the Kingdon equation was turned into the *damped Kingdon equation* given by

$$\ddot{r} + \gamma\dot{r} + [s - 2\eta\cos(2\tau)]\frac{1}{r} = 0. \quad (10)$$

The damped Kingdon equation (10) was integrated for  $\gamma=10^{-3}$  and several  $\eta$  values using a fourth-order Runge-Kutta scheme [4] with constant step size  $\Delta\tau = \pi/100$ . It was checked that this step size was sufficient to guarantee accurate solutions. Table I lists the results obtained for  $r_0$ ,  $r_0/\eta$ , and  $\xi$  for  $\eta$  values ranging from  $\eta=4$  to  $\eta=10$ . The value of  $r_0$  was taken as the time average of  $r$  over one complete micromotion cycle; the value of  $\xi$ , the micromotion amplitude, was defined as  $\xi = (r_{max} - r_{min})/2$ , where  $r_{max}$  and  $r_{min}$  are the maximal and the minimal distances of the ion from the filament, respectively. The column for the values of  $r_0/\eta$  was included in Table I since according to (8) we would expect this quantity to be constant and equal to

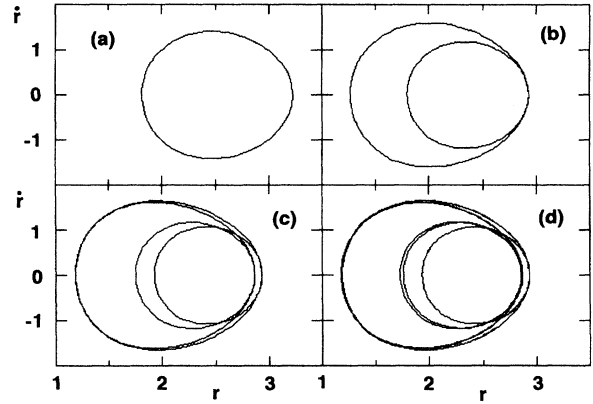


FIG. 1. Period-doubling bifurcations for a single ion in an ideal dynamic Kingdon trap. (a)  $q=3.5$ , simple period-1 limit cycle; (b)  $q=3.0$ , period-2 attractor; (c)  $q=2.92$ , period-4 attractor; (d)  $q=2.916$ , period-8 attractor.

$1/\sqrt{2}$ . Table I shows that  $\xi$  is very close to its pseudopotential estimate  $1/\sqrt{2}$ . The values of  $r_0/\eta$ , too, converge toward  $1/\sqrt{2}$ , as expected.

Since (10) is nonlinear and contains a drive term, there is a possibility for bifurcations and chaos to appear as a function of the control parameter  $\eta$ . Indeed, by using the same numerical scheme as was employed for generating Table I, several period-doubling bifurcations were identified in the parameter region  $\eta < 4$ . Figure 1(a) shows a phase-space portrait of the motion for  $\eta=3.5$ . The motion is regular. It is a limit cycle that corresponds to stable trapping at  $r_0 \approx 2.55$  with a micromotion amplitude of  $\xi \approx 0.7$ . Lowering the control parameter to  $\eta=3.0$  shows that the motion is now on a more complicated attractor [see Fig. 1(b)]. A period-doubling bifurcation of the limit cycle shown in Fig. 1(a) must have occurred between  $\eta=3.5$  and  $\eta=3.0$ . Figure 1(c) shows that at  $\eta=2.92$  the motion is on a period-4 attractor. Clearly another bifurcation must have occurred between  $\eta=3.0$  and  $\eta=2.92$ . Figure 1(d) shows the motion at  $\eta=2.916$  to be on a period-8 attractor. Again, a bifurcation must have occurred between  $\eta=2.92$  and  $\eta=2.916$ .

In order to exhibit the bifurcations more directly, (10) was integrated with  $\gamma=10^{-3}$  while slowly scanning the control parameter  $\eta$  from  $\eta=3.2$  to  $\eta=2.914$ . The whole  $\eta$  interval was traversed in  $2 \times 10^6$  cycles of the drive term in (10). The slow scanning speed is necessary in order to give the system time to relax. At 16 000 predetermined  $\eta$  values in the interval [2.914, 3.2] the values of  $r$  were obtained at the end of 16 successive cycles of the driving field in (10) and plotted vs the corresponding  $\eta$  value in a diagram. The result is shown in Fig. 2. The period-doubling bifurcations, whose presence was only indirectly concluded from the phase-space structures presented in Fig. 1, are now plainly visible. Focusing in on the bifurcation points, a total of five bifurcations was identified. They occur at  $\eta_1 \approx 3.124\,62$ ,  $\eta_2 \approx 2.938\,02$ ,  $\eta_3 \approx 2.917\,144$ ,  $\eta_4 \approx 2.914\,775$ , and  $\eta_5 \approx 2.914\,506$ . From Fig. 2 it might not be clear why, e.g., at  $\eta=2.92$ , there are only three branches of  $r$  and not four. The explanation is the following. Since the  $r$  values are plotted at integer multiples

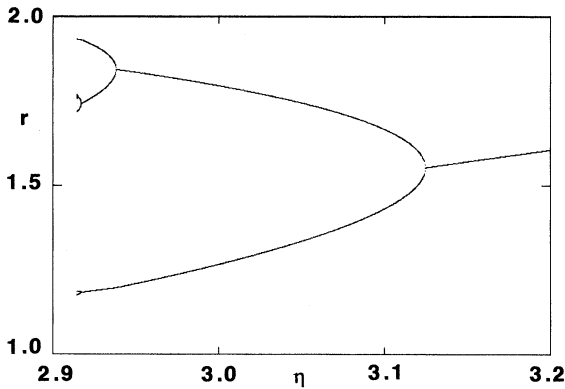


FIG. 2. Bifurcation diagram for a single charged particle stored in an ideal dynamic Kingdon trap.

of full cycles, there can be degeneracies in  $r$ . This is immediately clear from Fig. 1(b), for example. The two phase-space loops in Fig. 1(b), e.g., touch at maximum excursion.

The bifurcations shown in Fig. 2 resemble a period-doubling scenario [9]. Integrating (10) from cycle to cycle corresponds to a two-dimensional mapping  $[r(t), \dot{r}(t)] \rightarrow [r(t+\pi), \dot{r}(t+\pi)]$  that is approximately Hamiltonian because the damping constant is so small. The universal Feigenbaum constant for two-dimensional mappings is given by [10]

$$\delta = \lim_{j \rightarrow \infty} \frac{\eta_{j-1} - \eta_j}{\eta_j - \eta_{j+1}} \approx 8.72. \quad (11)$$

On the basis of the first five bifurcation points we obtain  $(\eta_1 - \eta_2)/(\eta_2 - \eta_3) = 8.9$ ,  $(\eta_2 - \eta_3)/(\eta_3 - \eta_4) = 8.8$ ,  $(\eta_3 - \eta_4)/(\eta_4 - \eta_5) = 8.8$ . These values are very close to the relevant Feigenbaum number.

The main question now is whether trapping, and in particular the period-doubling bifurcations, can be observed experimentally. Obviously we cannot have an infinitely long trap and any finite version will lead to field distortions. Also, it would be desirable to have a focusing force in the  $z$  direction, the direction of the trap's axis, in order to be able to observe the trapped ion at a specific location. In order to investigate this issue, the Laplace equation was solved numerically for a realistic dynamic Kingdon trap shown in Fig. 3. The trap is a finite-length version of the ideal dynamic Kingdon trap discussed above. The aspect ratio of the trap is  $a:b=1:2$ . The trap is equipped with two end caps that are held at the same potential as the outer cylinder of the trap. The line segments in Fig. 3 indicate the direction and the magnitude of the electric field inside the trap. It can be seen that due to the symmetry of the trap the radial field in the middle of the trap (at  $z=b/2$ ) is exactly in the radial direction. Therefore, at  $z=b/2$  and as far as the direction of the field is concerned, the realistic Kingdon trap behaves exactly like the ideal dynamic Kingdon trap. It was checked that not only the direction, but also the magnitude of the electric field in the vicinity of  $z=b/2$  behaves like  $1/r$  to a very good approximation. The question is whether exact  $1/r$  behavior is necessary to observe the period-doubling bifurcations dis-

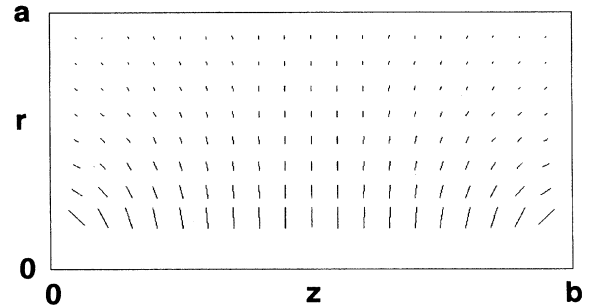


FIG. 3. Cross section of a realistic version of the dynamic Kingdon trap in the  $r$ - $z$  plane with aspect ratio  $a:b=1:2$ . The orientation of the line segments indicates the direction of the electric field; the length of the segments is proportional to the strength of the field.

cussed above. This question was answered by considering the *generalized Kingdon equation*

$$\ddot{r} + \gamma \dot{r} + [1 - 2\eta \cos(2\tau)] \frac{1}{r^\alpha} = 0, \quad (12)$$

where  $\alpha$  is a real constant. For  $\alpha \neq 1$  field distortions in the realistic trap can be modeled. The cases  $\alpha=0.9, 0.7, 0.5$ , and  $0.3$  were studied in some detail. In all these cases a period-doubling scenario was observed with the first period-doubling bifurcation occurring at  $\eta \approx 3.2, 3.4, 3.8, 4.6$ , respectively. This proves that, apart from a numerical shift in the location of the bifurcation points, the period-doubling scenario itself is astonishingly robust against field distortions. Figure 3 also shows that, due to the presence of the two end caps, the trap provides a focusing force in the  $z$  direction. Trapped particles will be found preferentially close to the center of the trap. Since the field in  $z$  direction vanishes exactly at  $z=b/2$ , the  $z$  field does not influence the  $r$  motion at  $z=b/2$ . Thus, the  $r$  motion decouples as assumed in the theory for the ideal dynamic Kingdon trap.

The dynamic Kingdon trap is remarkable in several respects. (i) In contrast to the Paul trap [2,3] the ac voltage does not produce a *focusing* effect but a *defocusing* effect. This is easily understood on general grounds. A trapped ion in an inhomogeneous ac field is a “low-field seeker” [3]. Since the field of a straight charged wire decreases with the distance from the wire, an applied ac voltage clearly tries to push an ion away from the central filament of the dynamic Kingdon trap. As shown above, this effect can be counterbalanced by a static attractive charge on the filament. The combined effects of attractive static charge and the repulsive effect of the ac voltage produce stable trapping. (ii) Since a trapped ion will hover above the filament, the micromotion cannot be eliminated even for a single trapped particle. For spectroscopic applications this is clearly a disadvantage. For applications in nonlinear dynamics this is an advantage since, as we saw above, even a single ion can exhibit interesting nonlinear effects on the basis of its never-vanishing micromotion. (iii) Interestingly, the equivalent of the “Mathieu equation” for single-ion trapping in the Paul trap

is nonlinear for the dynamic Kingdon trap. This allows us to scale out the Paul trap's  $a$  parameter [2–4] (proportional to the dc applied electric field). Thus, the single-ion dynamic Kingdon trap has only one control parameter  $\eta$ , which makes the discussion of nonlinear scenarios simpler. (iv) Another advantage of the dynamic Kingdon trap is its mechanical

simplicity. As shown in Fig. 3, a cylindrical arrangement with end caps and an aspect ratio of 1:2 is sufficient to observe the predicted effects.

It is a pleasure to thank Professor S. Fishman and Professor R. E. Prange for instructive discussions concerning the bifurcation scenario in the dynamic Kingdon trap.

- 
- [1] K. H. Kingdon, *Phys. Rev.* **21**, 408 (1923).  
[2] W. Paul, W. Osberghaus, and E. Fischer, *Forschungsber. Wirtsch. Verkehrsminist. Nordrhein Westfalen* **415**, 1 (1958).  
[3] W. Paul, *Rev. Mod. Phys.* **62**, 531 (1990).  
[4] *Handbook of Mathematical Functions*, Natl. Bur. Stand. Appl. Math. Ser. No. 55, edited by M. Abramowitz and I. A. Stegun (U.S. GPO, Washington, DC, 1965).  
[5] H. G. Dehmelt, in *Advances in Atomic and Molecular Physics*, edited by D. R. Bates and I. Estermann (Academic, New York, 1967), Vol. 3.  
[6] L. D. Landau and E. M. Lifschitz, *Mechanik* (Vieweg, Braunschweig, 1970).  
[7] R. Z. Sagdeev, D. A. Usikov, and G. M. Zaslavsky, *Nonlinear Physics* (Harwood Academic, Chur, 1988).  
[8] R. G. Lerner and G. L. Trigg, *Encyclopedia of Physics*, 2nd ed. (VCH, New York, 1991), p. 1239.  
[9] M. J. Feigenbaum, *Phys. Lett.* **74A**, 375 (1978); *J. Stat. Phys.* **19**, 25 (1978); **21**, 669 (1979).  
[10] S. Fishman, D. R. Grempel, and R. E. Prange, *Phys. Rev. A* **36**, 289 (1987).